New Horizons Journal of Basic and Applied Sciences, 2026, Vol. X, Iss. X, 77-88

DOI:10.62184/nhjbas.jnh20020261

Research Article

SCIENCE PARK PUBLISHER

New Horizons Journal of Basic and Applied Sciences

Formation constants and thermodynamic studies of copper complex with N^1-(2- hydroxybenzylidene) terephthalohydrazide

Elshaimaa G. Lawandi[1], Ahmed R. Abdellah[1,*], Shimaa Hosny[2] and Gamal A. Gouda[1]

[1] Department of Chemistry, Faculty of Science, Al-Azhar University, Assiut Branch, 71524, Assiut, Egypt

[2] Department of Chemistry, Faculty of Science, New Valley University, Alkharga 72511, Egypt

Received: 24, 11, 2025; Accepted: 02, 04, 2026; Published: 21, 05, 2026

Abstract

N^1-(2-hydroxybenzylidene) terephthalohydrazide (HL), a Schiff base, was synthesized and characterized using several analytical techniques. Potentiometric analysis of the complexation of Schiff base N^1-(2-hydroxy benzylidene) terephthalohydrazide (HL) with copper (II) was conducted at various temperatures (298–328 K) in an acidic medium (0.1 M HCl). The complexation of copper (II) with N^1-(2-hydroxy benzylidene) terephthalohydrazide in 0.1 M HCl was potentiometrically studied using Bjerrum method. The compositions of complexes were determined, and their stepwise formation constants were determined. The compositions of complexes were determined, and their stepwise formation constants were calculated. The complexes were shown to become less stable as the temperature increased. The thermodynamic functions of complexation were estimated.

Keywords: Potentiometric; Acid medium; Stability constant; Cu(II) complex; Thermodynamics

1. Introduction

The presence of many elements at trace levels that can be separated using complexing reagents makes characteristic stability constants a significant factor in predicting chemical processes, like isolation, extraction, and concentration methods [1]. Metal complexation involves bringing reacting molecules together to form an activated complex and directing polarized electrons from the ligands towards the metal [2, 3]. The formation constant and free energy change can provide insight into the relationship between ligand stability and basicity [4, 5]. The basicity and stability of ligands are enhanced by the bulkiness of groups. In order to determine the stability constant, the donor atoms, metal ion, nature of the ligand, ion radius, and charge of the metal in its oxidation state are all considered [6-8]. The oxidation-reduction titration using ligand redox electrodes is an available method for these studies that relies on oxygen atoms and their oxides. Several workers have reported their findings on metal-ligand stability constants [9-12]. Williams *et al.*, dissertation has been responsible for developing the field [13, 14]. Aqueous solution oxidation-reduction potentials for copper (II) complexes have not been widely published. According to a review, four potentials were found to be reasonably reliable, including 1:2 complexes with ammonia, imidazole, and ethylenediamine, and the sulphides [15]. Williams *et al.*, subsequently confirmed that the first three compounds had values within 0.02 V and also stated the potential for oxidizing or reducing 1:2 copper complexes in water with morpholine, 1,l0-o-phenanthrolines, piperidine, and 2,2'-bipyridyls [14]. The research uncovered a broad range of 1:2 copper complexes with 1,10-o-phenanthrolines and 2,2'-bispiridyls in 50% dioxane-water, but the correlation between these results and

DOI:10.62184/nhjbas.jnh20020261

Research Article

their potential in water is still a matter of contention. In the cases where aqueous values are known, they have a decrease of up to 131 mV, and there is a difference in the ranking order for bipyridyl complexes between the two solvents [16]. In addition, the redox potential measured by experiment can only be transformed into a standard potential (E_l^o) when the Cu(II) complexes are fully formed or when their stability constants are known. The E_f^* values given by Williams *et al.*, [14], where E_f^* is the formal redox potential for pairs of complexes at specified degrees of formation ($\bar{n}$), deviate from these potentials to an extent which depends on the consecutive stability constants of the complexes. When, as is often the case, Kl > K2, for the cuprous and the cupric complexes, E_f^* at $\bar{n}$ = 1 will be almost the same as E_l^o for the pair of 1:1 Cu(II)-L systems; but if, for example, in either series Kl = K2, the two values of E will be different because at $\bar{n}$ = 1 only one-third of the metal is present in the 1:1 complex. Given its relevance to biological systems, which undergo reversible oxidation-reduction reactions involving copper complexes, our study examines how complex formation with an organic ligand affects the redox potential of Cu(II) in HCl.

In this work, the stoichiometry and stability constants of complex formation of N^1-(2-hydroxybenzylidene) terephthalohydrazide ligand with Cu(II) ion in aqueous 0.1 M HCl at different temperatures were investigated. Furthermore, the thermodynamic characteristics of the complex formation were identified and discussed.

2. Experimental

2.1. Chemicals used and physical measurements

The chemical used in this study was of analytical reagent grade and was used directly without any further purification. We got salicylaldehyde, ethanol, iodine, and copper chloride dihydrate ($CuCl_2{\cdot}2H_2O$) from Sigma-Aldrich. Dimethyl terephthalate (Merk, Germany), hydrazine hydrate (Alpha Chem, China). A Shimadzu spectrophotometer with KBr pellets was used to record FT-IR spectra over 4000–400 cm^{-1}. In DMSO, ^{1}H NMR spectra were recorded using a Bruker 400 MHz NMR spectrometer. Using a R3003 voltage comparator with a platinum plate as the indicator electrode, potassium was titrated.

2.2. Preparation of N^1-(2-hydroxybenzylidene) terephthalohydrazide

Schiff base of N^1-(2-hydroxybenzylidene) terephthalohydrazide ligand (HL) was synthesized by condensation of 1,4-dicarbonyl-phenyl-dihydrazide (HY), (10 mmol, 1.94 g) with salicylaldehyde (SA), (10 mmol, 1.22 g) in ethanol at 60 °C. The reaction mixture was stirred for 4 hours. A solid compound was separated by filtration, washed by ethanol and recrystallized from dichloromethane and methanol (1:1) to give yellowish white crystals in a yield 89 % (Figure 1). The molecular structure of the formed Schiff base ($C_{15}H_{14}N_4O_3$) was established by the analytical data (Calc. (%): C 60.40, H 4.73, N 18.78, and found (%): C 61.32, H 4.43, N 19.92). FT-IR of the HL showed the absorption bands at 3400, 3217, 3057, 1660, and 1600 cm^{-1} due to phenolic -OH, -NH, CH–aromatic, C=O, and –C=C– groups, respectively (Figure 2). ^{1}H NMR spectrum (DMSO) of HL revealed the appearance of protons at δ (ppm) =3.9 (s, 2H), 6.8 - 7.7 (m, 4H), 8.1 - 8.2 (s, 4H), 8.7 (s, 2H sp^2), 9.6 (s, 1H),11.2 (s, 1H), 12.2 (s, 2H) ppm. (Figure 3).

2.3. Potentiometric studies

The redox system consisting of HL and its oxidized form was created by oxidizing a small portion of initial HL in 0.1 M HCl with a 0.5 mL (0.1 N) iodine solution. The stepwise complexation of Cu(II) with HL was studied using the Bjerrum method [17]. For this purpose, the redox system consisting of HL (0.00522 mole/l) and its oxidized form was titrated with a 0.00239 Cu(II) solution in 0.1 M HCl. The equilibrium ligand concentration and the formation function at each titration point were calculated by equations (1, 2) [13]:

$$log\,[L] = \frac{E_{initial} - E_i}{(1.9837x10^{-4})xT} + \log C_L^{initial} + \frac{1}{2} log \frac{V_{initial}}{V_{all}} \quad (1)$$

where $E_{initial}$ is the initial equilibrium potential of the oxidation-reduction system in the absence of copper (II); E_i is the equilibrium potential of each point of the titration. $C_L^{initial}$ is the initial analytical concentration of HL ligand; $V_{initial}$ / V_{all} is the ratio of the initial volume to the total volume of the system at each point of the titration: T is the temperature of the experiment in K. Determined at each point of the titration, the equilibrium concentration of the ligand was calculated as a function $\bar{n}$ by the formula:

$$\bar{n} = \frac{C_L - [L]}{C_{Cu(II)}} \quad (2)$$

DOI:10.62184/nhjbas.jnh20020261

Research Article

where $\bar{n}$ is the degree of formation from the titration curves of a HL with Cu(II) ion; C_L is the concentration of HL at each titration point; [L] is the equilibrium concentration of L at each titration; $C_{Cu(II)}$ is the concentration of copper (II) at each point of the titration. The stability constant values were calculated after analyzing the obtained results using an Excel program [18].

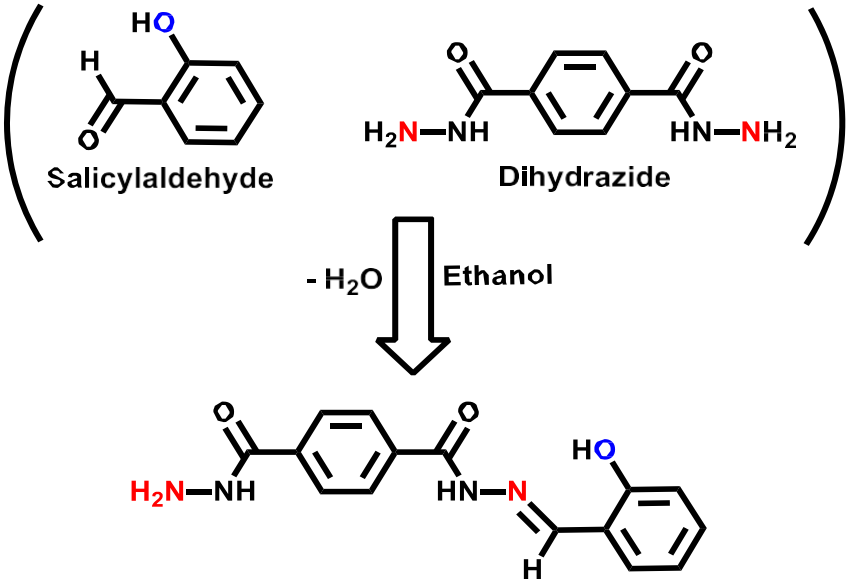

Figure 1. Synthesis of N^1-(2-hydroxybenzylidene) terephthalohydrazide.

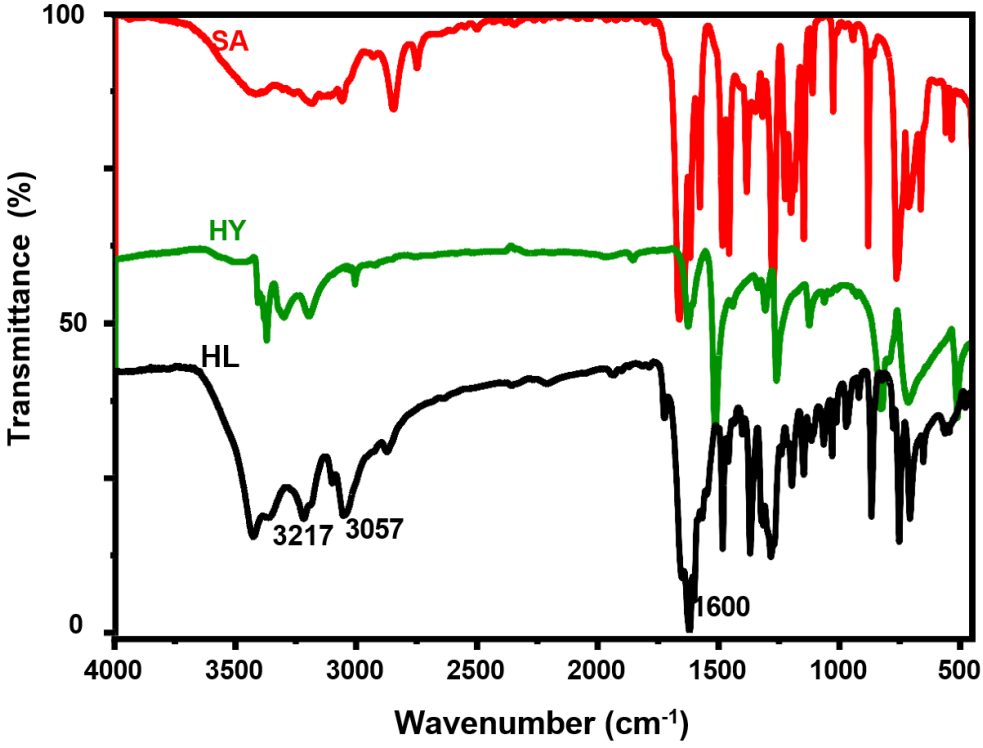

Figure 2. FT-IR spectra of the HY, SA, and Schiff base ligand HL.

New Horizons Journal of Basic and Applied Sciences, 2026, Vol. X, Iss. X, 77-88
DOI:10.62184/nhjbas.jnh20020261

Research Article

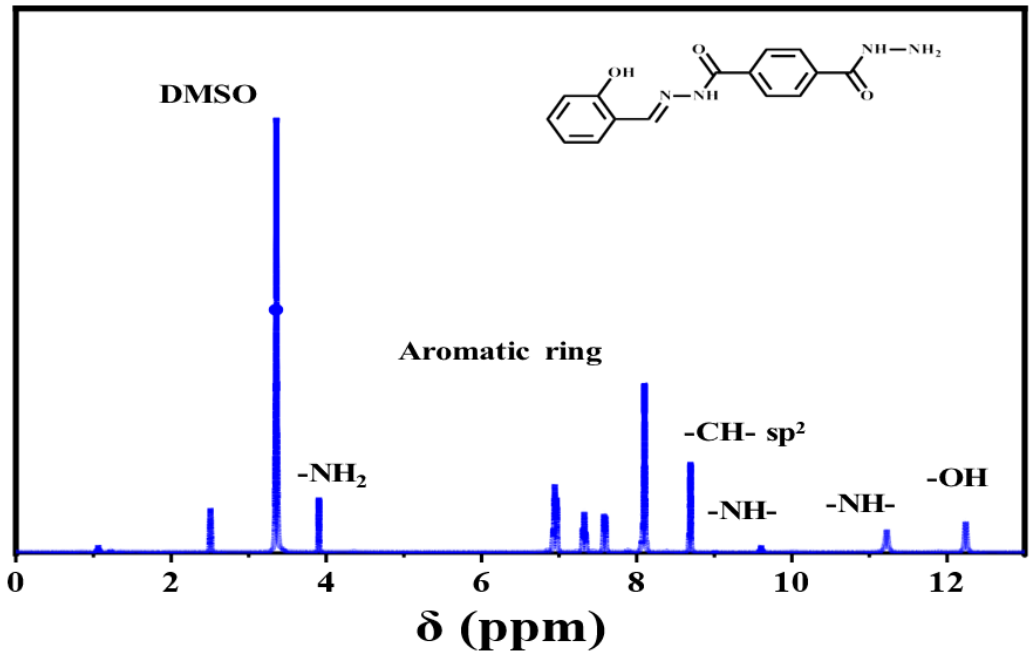

Figure 3. ^{1}H NMR spectrum of HL ligand in DMSO.

2.4. Thermodynamic characteristics

The thermodynamic properties of complex formation, such as enthalpy (ΔH°), Gibb's free energy (ΔG°), and entropy (ΔS°), are crucial for comprehending the different factors that may affect the complexes, including solute-solvent interactions and electronic and steric effects [19, 20]. The thermodynamic characteristics of the metal ion complexes at 298, 308, 318, and 328 K were examined. Equations (3) and (4) were utilized to determine the complicated degree of creation [21]:

$$\Delta G^{o} = \Delta H^{o} - T\Delta S^{o} \quad (3)$$

$$\log K_i = \frac{-\Delta H^{o}}{2.303\,R} + \frac{1}{T} \times \frac{\Delta S^{o}}{2.303\,R} \quad (4)$$

where R is the ideal gas constant (8.314 J/K mol). ΔH° and ΔS° were obtained from the intercept and slope of the plot of log K_i against 1/T.

3. Results and discussion

3.1. Potentiometric titration

According to studies, potentiometric titration causes the redox system's equilibrium potential to increase as the volume of added metal ions increases. There is no inclination to create hydroxo complexes because the titration produced no precipitates [22]. Potentiometric titration curves for the interaction between a Schiff base ligand (HL) and Cu(II) ions at various temperatures are displayed in Figure 4(a). Plotting the potential (mV) against the volume of Cu(II) titrant introduced reveals the redox and complex-formation characteristics of the Cu–Schiff base system. At the beginning (0–10 mL Cu(II) ion), the potential rises slowly corresponding to the initial coordination of Cu(II) ion to available donor sites (typically the azomethine nitrogen and phenolic oxygen) on the Schiff base; as more Cu(II) is added, the potential increases sharply indicating the formation of stable Cu(II)–HL ion complexes and a significant change in the oxidation–reduction equilibrium of the system. Each curve shows a gradual increase in the observed potential with the addition of Cu(II) ion solution. Finally, the potential levels off show that complex sites are saturated and the redox equilibrium is established. The potentiometric titration involves electron transfer between the Cu(II) ions and the Schiff base, which can act as a mild reducing agent through its electron-rich donor atoms (Cu(II) + HL ⇌ [Cu(II)L] + H^{+}). The complex formation increases the potential, as the oxidation state stabilizes Cu(II). During titration, the measured potential corresponds to the mixed redox potential of the Cu(II)/Cu(I) couple influenced by the ligand's coordination environment [23]. As Cu(II) ions are coordinated, the local environment

New Horizons Journal of Basic and Applied Sciences, 2026, Vol. X, Iss. X, 77-88
DOI:10.62184/nhjbas.jnh20020261

Research Article

around the metal changes, raising the redox potential until equilibrium is reached. Hence, the oxidation–reduction curves directly reflect the formation and stability of Cu(II)–Schiff base complexes, which are governed by electron-transfer and coordination equilibria.

In Figure 4(b), the formation titration curves of Cu(II)-HL ion complexes in 0.1 M HCl in the temperature range of 298-328 K are shown. Figure 4(b) represents the formation curves of Cu(II)–Schiff base (HL) complexes at different temperatures obtained by the Bjerrum method from potentiometric titration data in 0.1 M HCl medium. The plot shows the average number of ligands bound per metal ion ($\bar{n}$) on the *y-axis* versus log[L], the logarithm of the concentration of free ligand, on the *x-axis*.

The Bjerrum method is used to determine the formation (stability) constants (log K_i) of metal– ligand complexes in solution from potentiometric titration data [17]. It is based on calculating the average number of ligand molecules coordinated per metal ion ($\bar{n}$) at different free-ligand concentrations. The general equilibrium for the complexation process is:

$$Cu^{2+} + n\,HL \rightleftharpoons CuL_n^{(2-n)}$$

The relationship between $\bar{n}$ and [L] is used to extract the stability constants log K_1, log K_2, ….etc. Each curve represents how the average number of coordinated ligands changes as the free ligand concentration increases. The values of $\bar{n}$ range from 0 to ~3, showing that stepwise complexation occurs from mono- to bis- and possibly tris-chelated Cu(II) complexes. $\bar{n}$ values are around 2.5–3.0, indicating that at high Cu(II) concentration and low ligand concentration, most Cu(II) ions are fully coordinated, forming [CuL_2] or [CuL_3]- type complexes. $\bar{n}$ decreases gradually as the ratio of free ligand increases, showing stepwise dissociation of complexes. The system transitions between $CuL_2 \rightarrow CuL \rightarrow Cu^{2+}$, reflecting the equilibrium shifts as more ligand is added and complex stability changes. $\bar{n}$ approaches zero, meaning free ligand dominates, and the concentration of coordinated complexes becomes small. Through the calculated equilibrium log K values (Table 1) provided at 298 K, we computed β, the overall stability constant ($\beta = K1 \cdot K_2 \cdot K_3$) [24]. Table 1 presents the stepwise stability constants (log K_1, log K_2, log K_3) for the successive formation of Cu(II)–HL complexes in 0.1 M HCl at different temperatures (298–328 K).

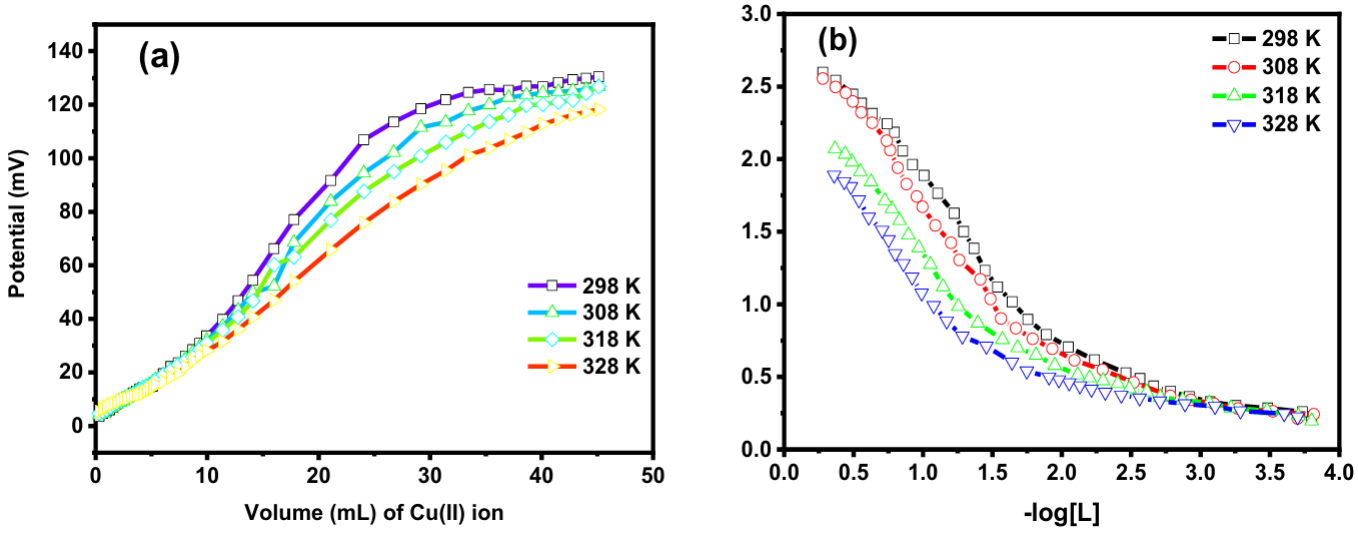

Figure 4. Potentiometric and formation titration curves (a) and (b) respectively, of 25 mL of Schiff base HL (5.22×10^{3} M) with mL add of Cu(II) ion (2.39×10^{3} M) in 0.1 M HCl at various temperatures.

New Horizons Journal of Basic and Applied Sciences, 2026, Vol. X, Iss. X, 77-88
DOI:10.62184/nhjbas.jnh20020261

Research Article

Table 1. Stepwise stability constants of Cu(II)-HL ion complexes in 0.1 M HCl.

Temperature (K)	log K_1 $[CuL(H_2O)_5]^+$	log K_2 $[CuL_2(H_2O)_4]$	log K_3 $[CuL_3(H_2O)_3]^-$	log β $\beta = K_1 \cdot K_2 \cdot K_3$
298	4.24	2.34	1.46	1.10×10^8
308	3.88	2.26	1.27	2.57×10^7
318	3.55	2.05	1.15	5.62×10^6
328	3.23	1.78	0.82	6.76×10^5

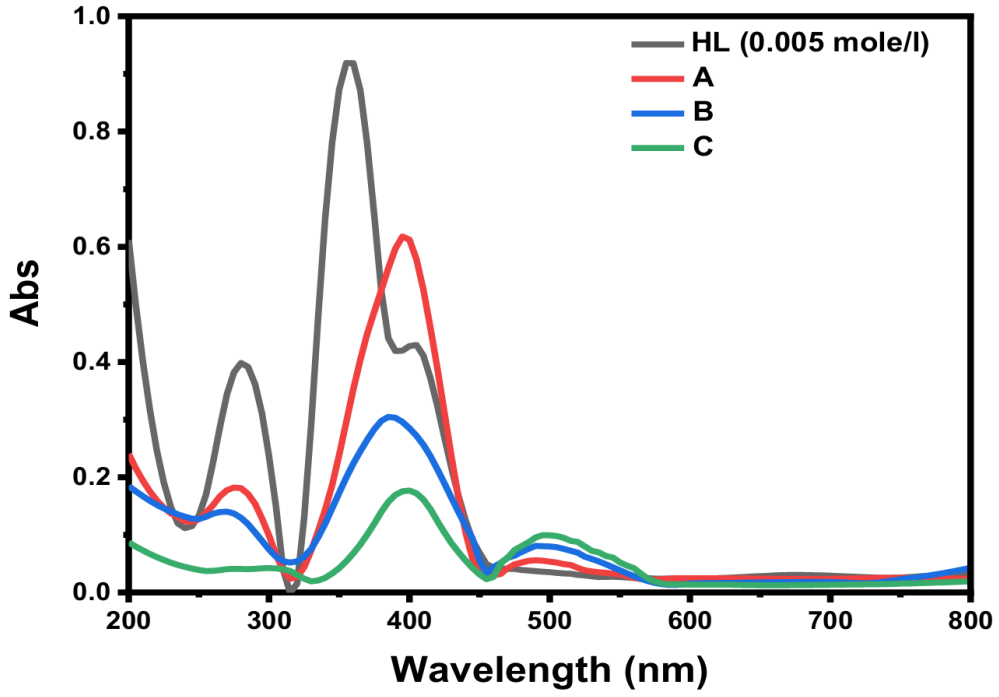

Figure 5. UV-vis absorption spectra of the Schiff base ligand (HL) and Cu(II) ion solution at the start and finish of the potentiometric titration (where (A) represents the start of the Cu(II) ion addition to the HL, (B) shows the center of the potentiometric, and (C) represents the end of the potentiometric.

The formation of Cu(II)–HL complexes occurs stepwise as follows:

$$Cu^{2+} + HL \rightleftharpoons [CuL(H_2O)_5]^+ K_1$$

$$[CuL(H_2O)_5]^+ + HL \rightleftharpoons [CuL_2(H_2O)_4] K_2$$

$$[CuL_2(H_2O)_4] + HL \rightleftharpoons [CuL_3(H_2O)_3]^- K_3$$

Each step corresponds to the replacement of coordinated water molecules by the Schiff base ligand (HL) [25, 26]. This decreasing trend (log K_1 > log K_2 > log K_3) is typical for stepwise complex formation and is explained by a) Statistical effect: the first ligand coordinates easily with Cu(II), but subsequent ligands must bind to an already partially occupied coordination sphere. b) Steric hindrance: as more bulky Schiff base ligands bind, less space is available for additional coordination. c) Electrostatic repulsion: the complex becomes more negatively charged, it is less favorable for further anionic or neutral ligands to approach.

Figure 5 presents the UV–visible absorption spectra of the Schiff base ligand (HL, 0.005 mol L^{-1}) and its Cu(II) system recorded at different stages of the potentiometric titration, over the wavelength range 200–800 nm. The free ligand HL exhibits intense absorption bands in the UV region (280 nm), which can be attributed to π→π* transitions of the aromatic rings and n→π* transitions associated with the azomethine (–C=N–) group. An additional strong band appears in the near-UV/visible region around 360 nm, characteristic of extended conjugation in the Schiff base structure. Curve A (start of

DOI:10.62184/nhjbas.jnh20020261

Research Article

Cu(II) addition) shows noticeable changes in both intensity and position of the ligand bands, indicating the initial coordination of Cu(II) ions with HL. The increase in absorbance and slight bathochromic shifts suggest involvement of the azomethine nitrogen and, possibly, the phenolic oxygen atoms in metal binding, leading to ligand-to-metal charge-transfer (LMCT) contributions. Curve B (middle of the potentiometric titration) displays further modulation of the spectral features, with reduced intensity of the free- ligand bands and the emergence of broader bands in the 350–450 nm region. This behavior is consistent with the progressive formation of Cu(II)–HL complexes and their redistribution among different complex species in solution. Curve C (end of the potentiometric titration) shows the lowest overall absorbance in the UV region and a weak, broad band extending into the visible region (~450–550 nm), which can be assigned to d–d transitions of Cu(II) in a distorted octahedral or square-planar coordination environment. The stabilization of the spectral profile at this stage indicates completion of complex formation. Overall, the systematic spectral changes from HL to A, B, and C clearly confirm complexation between the Schiff base ligand and Cu(II) ions, in good agreement with the potentiometric titration results and supporting the stepwise formation of Cu(II)–HL species in solution.

Table 2 compares the formation species of the Cu(II) ion with different organic ligands in aqueous and non-aqueous media by potentiometric titration.

3.2. Thermodynamic functions

The van't Hoff equation was used to determine the values of free energy (ΔG°), enthalpy (ΔH°), and entropy changes (ΔS°) that accompany complex reactions at 298, 308, 318, and 328 K (Table 3) [33]. The enthalpy change (ΔH°) for the dissociation or complexation process was assessed by evaluating the slope of the plot (log K_i vs. 1/T), as indicated in Figure 6. The ΔG° values are negative (spontaneous formation) for all three steps at the temperatures shown (e.g. $\Delta G°_1 \approx -24.22$ kJ·mol^{-1} at 298 K, $\Delta G°_2 \approx -15.34$ kJ·mol^{-1}, $\Delta G°_3 \approx -15.34$ kJ·mol^{-1}) [21, 34]. The magnitude of ΔG° decreases with increasing temperature, so each step becomes less favorable at higher T. This matches the speciation plots and the observed reduction of log K with temperature. Negative ΔH° values indicate exothermic formation. The first coordination step is much more exothermic than the second and third. That indicates the strongest metal–ligand bond formation occurs on the first ligand addition (large favorable bonding/chelate energy), while further ligand additions release less heat (weaker incremental bond energy, increasing steric/electrostatic penalties) [35, 36].

Table 2. The formation species of Cu(II)-L species in different media.

Organic ligand	Medium	The species [Cu(II):L] ratio	Ref.
1,2-bis(2-hydroxyphenyl)- naphtaldiimine	Water or acetonitrile	Cu(II)-L, Cu(II)-LH, Cu(II)-LOH and Cu(II)-L_2	[27]
N,N′-o-phenylenebis- (salicylideneimine)	Water–ethanol (90:10 v/v) mixture	[Cu(II)L], and $[Cu(II)HL]^+$	[28]
2-aminomethylthiophenyl-4- bromosalicylaldehyde	50% (v/v) DMSO–water	[Cu(II)L] and $[Cu(II)L_2]$	[29]
(*E*)-1-[(2,4-dichlorophenylimino)-methyl]naphthalen-2-ol,	Aqueous-ethanol solutions[ethyl alcohol (30%) and water (70%)	Cu(II)-L, Cu(II)- LH, Cu(II)-LOH and Cu(II)-L_2	[30]
1-methyl-2-mercaptoimidazole	7 M HCl	Cu(II)-L, Cu(II)-L_2, Cu(II)-L_3 and Cu(II)-L_4	[31]
2- mercaptobenzothiazole	1 M HCl	Cu(II)-L, and Cu(II)-L_2	[32]
N^1-(2-hydroxybenzylidene)- terephthalohydrazide	0.1 M HCl	Cu(II)-L, Cu(II)- L_2, and Cu(II)-L_3	This work

DOI:10.62184/nhjbas.jnh20020261

Research Article

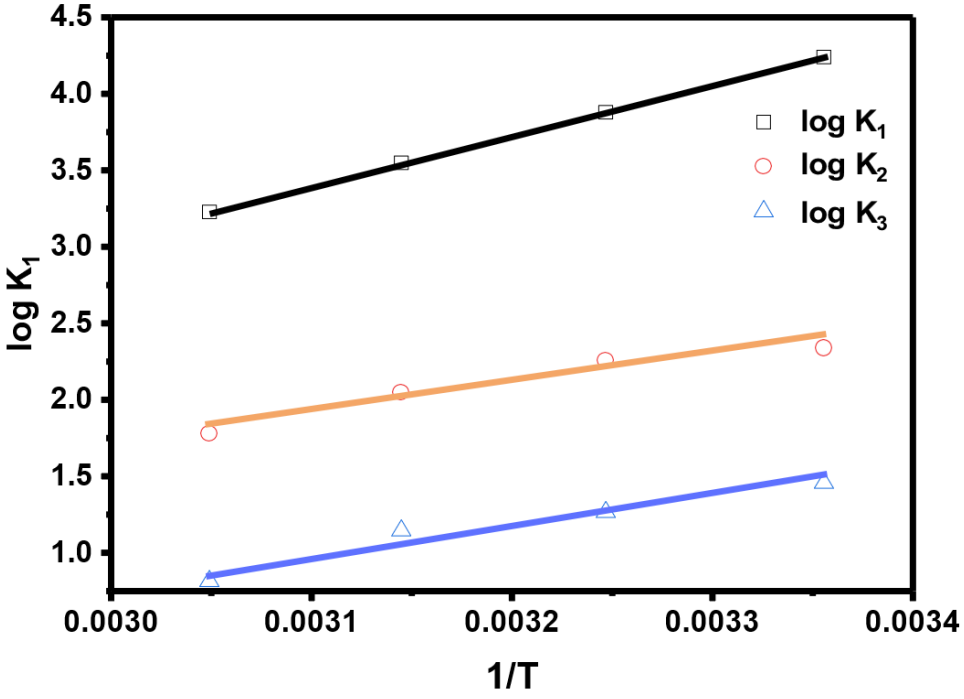

Figure 6. Vant Hoff plot of log K_i of Cu(II) ion complexes of HL ligand against 1/T.

Table 3. The values of thermodynamic parameter ΔG°, ΔH°, and ΔS° of formation Cu(II)-HL species corresponding to $[CuL(H_2O)_5]^+$, $[CuL_2(H_2O)_4]$, and $[CuL_3(H_2O)_3]^-$ compounds.

Temperature (K)	-ΔG° (kJ.mol^{-1})			- ΔH° (kJ.mol^{-1})			- ΔS° (J.mol–1.K^{-1})		
	ΔG°$_1$ (1:1)	ΔG°$_2$ (1:2)	ΔG°$_3$ (1:3)	ΔH°$_1$ (1:1)	ΔH°$_2$ (1:2)	ΔH°$_3$ (1:3)	ΔS°$_1$ (1:1)	ΔS°$_2$ (1:2)	ΔS°$_3$ (1:3)
298	24.22	15.34	15.34	62.88	35.12	37.99	129.82	66.37	76.01
308	22.94	12.61	12.62				127.87	73.05	82.37
318	21.65	10.79	10.79				129.77	76.49	85.52
328	21.65	7.22	7.22				129.87	85.05	93.80

In Table 3, the ΔS° is negative for all steps (examples at 298 K: $\Delta S°_1 \approx -129.8$ J·mol^{-1}·K^{-1}, $\Delta S°_2 \approx -66.4$ J·mol^{-1}·K^{-1}, $\Delta S°_3 \approx -76.0$ J·mol^{-1}·K^{-1}). A negative ΔS° indicates overall ordering on complexation (loss of translational/rotational freedom, more rigid coordination sphere). Any release of water molecules upon coordination does not overcome the net loss of degrees of freedom; thus, the entropy change is unfavorable. The largest entropy penalty occurs in the first step, consistent with the large structural/solvation reorganization that occurs when the first ligand displaces coordinated water and forms the primary coordinate bond [37]. Here, ΔH° is negative (favorable) while ΔS° is negative (unfavorable). At low T, the exothermic ΔH° term dominates, and ΔG° is substantially negative (spontaneous). As T increases, the $-T\Delta S°$ term becomes less favorable (because $\Delta S° < 0$, $-T\Delta S°$ is positive), so ΔG° becomes less negative, and complexes destabilize with temperature. This quantitatively explains the decrease of log K with T and the shifts in the species distribution plots [24, 37, 38].

New Horizons Journal of Basic and Applied Sciences, 2026, Vol. X, Iss. X, 77-88
DOI:10.62184/nhjbas.jnh20020261

Research Article

3.3. The distribution diagrams

In Figure 7, the species-distribution plot shows which copper species are present (and at what %) as the free-ligand concentration changes. They were obtained using the SPE program [39, 40]. The four curves (labelled X_0, X_1, X_2, X_3) are the percent of total copper present as: X_0 = free Cu^{2+} (or hydrolysed Cu species plus water-coordinated Cu), X_1 = the 1:1 Cu–HL complex, X_2 = the 1:2 Cu–$(HL)_2$ complex, and X_3 = the 1:3 Cu–$(HL)_3$ complex. Horizontal axis: ligand concentration plotted as log [L] (increasing ligand to the right). Vertical axis: fraction (percent) of total copper present as each species. At very low [L] (left side), there isn't enough ligand, so X_0 (free Cu) is near 100%. As [L] rises, the first ligand binds and X_1 grows, producing a bell-shaped curve: it rises when enough ligand is present to form 1:1 and falls once more ligand drives formation of 1:2 and 1:3 species. With still more ligand, X_2 becomes dominant, then finally at very large [L], X_3 dominates. Each complex has a concentration window where it is the major species, which is why each complex curve is a peak (or a hump) rather than a monotonic increase. The intersection points of two curves (where their percentages are equal) correspond to ligand concentrations at which the equilibrium strongly shifts from one stoichiometry to the next; these points are controlled by the stepwise stability constants (K_1, K_2, K_3) and total concentrations (mass balance).

Overall shift of the curves with temperature from 308 to 318 K that higher ligand concentrations are required to achieve the same degree of complexation. In other words, at 318 K, the peaks for the Cu(II)–HL complexes occur at somewhat larger log [L] than at 308 K. This shift indicates that the complexes are less stable at the higher temperature (consistent with the numerical log K values you gave earlier, which decrease with rising T). If formation is exothermic, raising T pushes equilibria toward dissociation, so you need more ligand to form the same fraction of complex. Relative domains shrink for higher complexes at higher T: the ligand range where X_1 and X_3 are the major species becomes narrower (and the maxima lower) at higher T, reflecting the reduced stability of successive ligand additions as temperature increases. The plot used the specified initial totals (≈2.39×10^{-3} M Cu and 2.30×10^{-3} M HL). Because the total ligand is of the same order as the metal, you will not reach the 100% asymptotic X_3 unless you go to very large free-L (i.e., a large external ligand excess). The mass balances mean the absolute heights and positions of the peaks depend on those starting totals as well as the K.

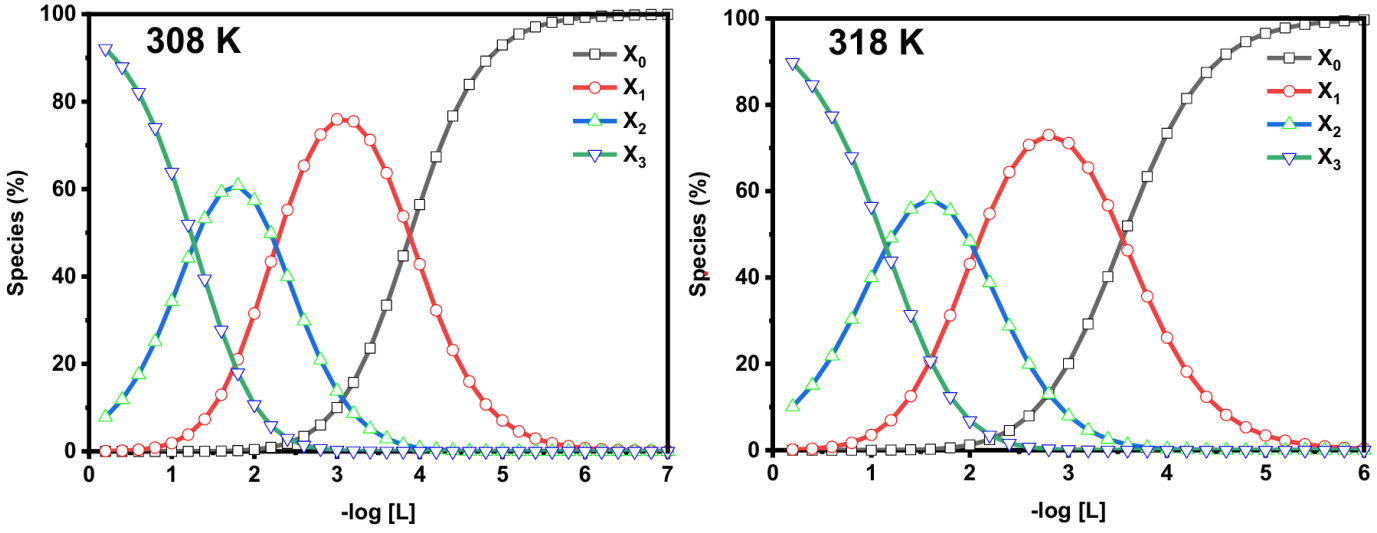

Figure 7. Species distribution curves of Cu(II)-HL ion complexes as a function of –log [L] in 0.1 M HCl at 308 and 318 K.

DOI:10.62184/nhjbas.jnh20020261

Research Article

4. Conclusion

The Cu(II)–HL complexes exhibit normal stepwise complexation behavior, with decreasing stability constants ($K_1 > K_2 > K_3$). The decrease of log K with temperature confirms that the formation of these complexes is exothermic and enthalpy-driven. The first complex (1:1) is the most stable due to the strong coordination of the Schiff base donor atoms (like N and O), while subsequent additions are hindered sterically and electrostatically. The distribution plots show the expected sequence (free Cu → 1:1 → 1:2 → 1:3) as the ligand increases. Increasing temperature shifts the equilibria toward dissociation (peaks shift to higher [L] values and higher complexes are less populated), consistent with the measured decrease in log K_1–K_3 with temperature. All three formation steps are spontaneous ($\Delta G° < 0$) and exothermic ($\Delta H° < 0$), but each has a negative entropy change ($\Delta S° < 0$). The process is therefore enthalpy-driven and becomes progressively less favorable at higher temperatures because the unfavorable entropy term becomes increasingly important ($\Delta G°$ becomes less negative). The first (1:1) step is both the most exothermic and has the largest (most negative) entropy penalty, producing the largest driving force at low T; successive ligand additions are noticeably weaker. Thermodynamically, the formation is therefore enthalpy-driven (bond formation) and entropy-penalized (ordering on binding).

Funding

This work was funded by a Master's Degree Thesis entitled "Green synthesis of nano coordination complexes derived from dihydrazide terephthalate, characterization and application".

Conflict of interest

The authors declare that they have no known competing financial interests or personal relationships that could have appeared to influence the work reported in this paper.

Ethics approval and consent to participate

This work has been done under a protocol approved by the Faculty of Science, Al-Azhar University, Assiut, Ethical Committee Review Board which confirmed that all experiments were performed in accordance with relevant guidelines and regulations of Al-Azhar University (No. AZHAR3/2024).

Authorship contributions

Conceptualization, Methodology, Software, Data curation: El.G.L., A.R.A., S.H., G.A.G. Visualization, Investigation: El.G.L.

Supervision: A.R.A., S.H., G.A.G.

Writing- Reviewing and Editing: A.R.A., S.H., G.A.G.

Author information

Corresponding authors: Ahmed R. Abdellah*

E-mail: AhmedR.Abdellah@azhar.edu.eg

ORCID iD: 0000-0002-7102-8620

Data availability

Data will be available on request.

References

[1] Feldmann, J., Salaün, P., & Lombi, E. (2009). Critical review perspective: elemental speciation analysis methods in environmental chemistry–moving towards methodological integration. Environmental Chemistry, *6*(4), 275-289. https://doi.org/10.1071/EN09018

[2] Al-Farhan, B. S., Gouda, G. A., Farghaly, O., & Khalafawy, A. K. E. L. (2019). Potentiometeric study of new Schiff base complexes bearing morpholine in ethanol-water medium with some metal ions. International Journal of Electrochemical Science, 14(4), 3350- 3362. https://doi.org/10.20964/2019.04.38

[3] Al-Saidi, H. M., Gouda, G. A., & Farghaly, O. (2020). Potentiometric study of a new Schiff base and its metal ion complexes: preparation, characterization and biological activity. International Journal of Electrochemical Science, 15(11), 10785-10801. https://doi.org/10.20964/2020.11.06

[4] Xu, H., Xu, D. C., & Wang, Y. (2017). Natural indices for the chemical hardness/softness of metal cations and ligands. American Chemical Society omega, 2(10), 7185-7193. https://doi.org/10.1021/acsomega.7b01039

[5] Esmaielzadeh, S., & Mashhadiagha, G. (2017). Formation constants and thermodynamic parameters of bivalent Co, Ni, Cu and Zn complexes with Schiff base ligand: Experimental and DFT calculations. Bulletin of the Chemical Society of Ethiopia, 31(1), 159-170. https://doi.org/10.4314/bcse.v31i1.14

[6] Grochala, W. (2017). The generalized maximum hardness principle revisited and applied to atoms and molecules.

DOI:10.62184/nhjbas.jnh20020261

Research Article

Physical Chemistry Chemical Physics, 19(46), 30964-30983. https://doi.org/10.1039/C7CP03101G

[7] Law, S. K. (2024). Role of ligand design on the stability of metal complexes and its catalytic properties-A mini-review. Biointerface Research in Applied Chemistry, 14, 64. https://doi.org/10.33263/BRIAC143.064

[8] Richens, D. T. (2005). Ligand substitution reactions at inorganic centers. Chemical Reviews, 105(6), 1961-2002. https://doi.org/10.1021/cr030705u

[9] Solov'Ev, V., & Tsivadze, A. (2023). Prediction of stability constants of metal-ligand complexes using thermodynamic radii of metal ions. Comments on Inorganic Chemistry, 43(1), 16-33. https://doi.org/10.1080/02603594. 2022.2087637

[10] Kanahashi, K., Urushihara, M., & Yamaguchi, K. (2022). Machine learning-based analysis of overall stability constants of metal–ligand complexes. Scientific Reports, 12(1), 11159. https://doi.org/10.1038/s41598-022-15300-9

[11] Agrawal, Y., & Patel, D. (1986). Thermodynamic proton-ligand and metal-ligand stability constants of some drugs. Journal of Pharmaceutical Sciences, 75(2), 190-192. https://doi.org/10.1002/jps.2600750219

[12] Gutten, O., & Rulisek, L. (2013). Predicting the stability constants of metal-ion complexes from first principles. Inorganic Chemistry, 52(18), 10347-10355. https://doi.org/10.1021/ic401037x

[13] Amindzhanov, A., Manonov, K., Kabirov, N., & Abdelrahman, G. A. H. (2016). Copper (II) complexation with 1-methyl-2-mercaptoimidazole in 7 M HCl. Russian Journal of Inorganic Chemistry, 61(1), 81-85. https://doi.org/10.1134/S0036023616010034

[14] James, B., & Williams, R. (1961). 383. The oxidation–reduction potentials of some copper complexes. Journal of the Chemical Society (Resumed), 2007-2019. https://doi.org/10.1039/JR9610002007

[15] Perrin, D., & Hawkins, C. (1965). The oxidation-reduction potentials of copper complex ions. In Electrochemistry, (Elsevier), pp. 115- 123. https://doi.org/10.1016/B978-1-4831-9831-6.50015-1

[16] Bond, A. M., & Haga, M. (1986). Spectrophotometric and voltammetric characterization of complexes of bis (2, 2'-bipyridine)(2, 2'-bibenzimidazole) ruthenium and-osmium in oxidation states II, III, and IV in acetonitrile/water mixtures. Inorganic Chemistry, 25(25), 4507-4514. https://doi.org/10.1021/ic00245a012

[17] Bjerrum, J. (1941). Metal amine formation in aqueous solution. Haase, Copenhagen.

[18] Sarac, B., & Hadzi, S. (2021). Analysis of protonation equilibria of amino acids in aqueous solutions using Microsoft Excel. Journal of Chemical Education, 98(3), 1001 1007. https://doi.org/10.1021/acs.jchemed.0c01144

[19] Solomonov, B. N., & Yagofarov, M. I. (2025). The relationship between the Gibbs energies and enthalpies of hydrogen bonding and charge-transfer complex formation in non-electrolytes solutions. Is it a rule?. Journal of Molecular Liquids, 424, 127053. https://doi.org/10.1016/j.molliq.2025.127053

[20] Abdel-Moez, M. S., El-Wafa, S. A., Sleem, H. S., & El-Shetary, B. A. (1989). Thermodynamics, stability constants and spectrophotometric studies of complexes of trivalent lanthanides and some divalent metals with 3- [α- (o-hy. Thermochimica Acta, 149, 317-329. https://doi.org/10.1016/0040-6031(89)85292-X

[21] Kubicek, V., Bohmova, Z., Sevcikova, R., Vanek, J., Lubal, P., Polakova, Z., ... & Hermann, P. (2018). NOTA complexes with copper (II) and divalent metal ions: kinetic and thermodynamic studies. Inorganic Chemistry, 57(6), 3061-3072. https://doi.org/10.1021/acs.inorgchem.7b02929

[22] Tünay, O., & Kabdaşli, N. (1994). Hydroxide precipitation of complexed metals.
Water Research, 28(10), 2117-2124. https://doi.org/10.1016/0043-1354(94)90022-1

[23] Ambundo, E. A., Deydier, M. V., Grall, A. J., Aguera-Vega, N., Dressel, L. T., Cooper, T. H., ... & Rorabacher, D. B. (1999). Influence of coordination geometry upon copper (II/I) redox potentials. Physical parameters for twelve copper tripodal ligand complexes. Inorganic Chemistry, 38(19), 4233-4242. https://doi.org/10.1021 /ic990334t

[24] Gouda, G. A. H., & Ali, G. A. M. (2017). Potentiometric study of rhenium (V) complex formation with azathioprine and ceftriaxone. Malaysian Journal of Analytical Sciences, 21, 1266-1275. https://doi.org/10. 17576/mjas-2017-2106-08

[25] Williamson, M. P. (2013). Using chemical shift perturbation to characterise ligand binding. Progress in Nuclear Magnetic Resonance Spectroscopy, 73, 1-16. https://doi.org/10.1016/j.pnmrs.2013.02.001

[26] Angell, C. A., & Gruen, D. M. (1966). Octahedral-Tetrahedral coordination equilibria of nickel (II) and copper (II) in concentrated aqueous electrolyte solutions. Journal of

DOI:10.62184/nhjbas.jnh20020261

Research Article

the American Chemical Society, 88(22), 5192-5198. https://doi.org/10.1021/ja00974a029

[27] Shokrollahi, A., Ghaedi, M., & Ghaedi, H. (2013). Potentiometric and spectrophotometric studies of copper (II) complexes of some ligands in aqueous and nonaqueous solution. Journal of the Chinese Chemical Society, 54(4), 933-940. https://doi.org/0.1002/jccs.200700134

[28] Belaid, S., Djebbar, S., Benali-Baitich, O., Khan, M., & Bouet, G. (2007). Complex formation between manganese (II), cobalt (II), nickel (II), copper (II) and a series of new ligands derived from N, N′-O-phenylenebis (salicylideneimine). Comptes Rendus. Chimie, 10(7), 568-572. https://doi.org/10.1016/j.crci.2006.09.012

[29] El-Sherif, A. A., & Eldebss, T. M. (2011). Synthesis, spectral characterization, solution equilibria, in vitro antibacterial and cytotoxic activities of Cu (II), Ni (II), Mn (II), Co(II) and Zn (II) complexes with Schiff base derived from 5-bromosalicylaldehyde and 2-aminomethylthiophene. Spectrochimica Acta Part A: Molecular and Biomolecular Spectroscopy, 79(5), 1803-1814. https://doi.org/10.1016/j.saa. 2011.05.062

[30] Al-Obaidi, F. N., Atabey, H., Macit, M., & Sari, H. (2023). Potentiometric study of the dissociation constants of some schiff bases from ortho-Hydroxynaphthaldehyde and 2, 4-substituted aniline and stability constants of their Cu (II) complexes in mixed solvents. Russian Journal of General Chemistry, 93(Suppl 4), S858-S867. https://doi.org/10. 1134/s1070363223170024

[31] Amindzhanov, A. A., Manonov, K. A., Kabirov, N. G., & Abdelrahman, G. A. H. (2016). Copper (II) complexation with 1-methyl-2-mercaptoimidazole in 7 M HCl. Russian Journal of Inorganic Chemistry, 61(1), 81-85. https://doi.org/10.1134/s0036023616010034

[32] Gouda, G. A., & Abdelaal, K. (2015). Potentiometric and thermodynamic studies of 2-mercaptobenzothiazole complexes with selected metal ions. Assiut University Journal of Multidisciplinary Scientific Research, 24, 91-98. https://doi.org/10.21608/aunj.2015.222243

[33] Maridevarmath, C., & Malimath, G. (2020). Studies on the effect of temperature on dielectric relaxation, activation energy (ΔG*), enthalpy (ΔH*), entropy (ΔS*) and molecular interactions of some anilines, phenol and their binary mixtures using X- band microwave bench. The Journal of Chemical Thermodynamics, 144, 106068. https://doi.org/10.1016/j. jct.2020.106068

[34] Bandyopadhyay, S., Mukherjee, G., & Drew, M. (2006). Equilibrium studies on mixed ligand complex formation of Co (II), Ni (II), Cu (II) and Zn (II) with N-(2- hydroxybenzyl)-l-histidine (H2hb-l-his) and typical N, N donor ligands: Crystal structure of [Ni (hb-l-his)(bipyridine)]. H_2O complex. Inorganica chimica acta, 359(10), 3243-3251. https://doi.org/10.1016/j.ica.2006.03.031

[35] Hughes, A. K., & Wade, K. (2000). Metal–metal and metal–ligand bond strengths in metal carbonyl clusters. Coordination Chemistry Reviews, 197(1), 191-229. https://doi.org/10.1016/S0010-8545(99)00208-8

[36] Guan, H., Harris, C., & Sun, S. (2023). Metal–ligand interactions and their roles in controlling nanoparticle formation and functions. Accounts of Chemical Research, 56(12), 1591-1601. https://doi.org/10.1021/acs.accounts. 3c00156

[37] Gouda, G., Shatat, M., Seaf Elnasr, T., & Abdallah, M. (2013). Potentiometric and thermodynamic investigation of rhenium(V) complexes with 1-methyl -2-mercaptoimidazole. Al-Azhar Bulletin of Science, 24(2-A), 141-148.

[38] Abd El-Karim, A. T., & El-Sherif, A. A. (2016). Potentiometric, equilibrium studies and thermodynamics of novel thiosemicarbazones and their bivalent transition metal (II) complexes. Journal of Molecular Liquids, 219, 914-922. https://doi.org/10.1016/j.molliq.2016.04.005

[39] Mansour, F. R., & Danielson, N. D. (2012). Ligand exchange spectrophotometric method for the determination of mole ratio in metal complexes. Microchemical Journal, 103, 74-78. https://doi.org/10.1016/j.microc.2012.01.008

[40] El-Mottaleb, M., Gouda, G. A., Badawy, N., & Kamale, F. H. (2018). Potentiometric and theoretical Studies of 2-((4-Morpholinobenzylidene) amino) phenol with some transition elements. Assiut University Journal of Multidisciplinary Scientific Research, 47, 51-65. https://doi.org/10.21608/aunj.2018.221242